Charge transfer resistance reduction by the interlayer distance expansion of Ni-Al layered double hydroxide for nickel-metal hydride battery anode

Maki, Hideshi

Inoue, Masayoshi

Mizuhata, Minoru

Charge Transfer Resistance Reduction by the Interlayer Distance Expansion of Ni-Al Layered Double Hydroxide for Nickel-metal Hydride Battery Anode

Hideshi Maki[a,b*], Masayoshi Inoue[b], and Minoru Mizuhata[b]

[a]Center for Environmental Management, Kobe University, 1-1 Rokkodai-cho, Nada-ku, Kobe 657-8501, Japan

[b]Department of Chemical Science and Engineering, Graduate School of Engineering, Kobe University, 1-1 Rokkodai-cho, Nada-ku, Kobe 657-8501, Japan

CORRESPONDING AUTHOR FOOTNOTE

Authors to whom correspondence should be addressed. E-mail: maki@kobe-u.ac.jp

Keywords:

LDH; Liquid phase deposition; LPD; NiMH; Nickel hydride;

ABSTRACT

The Ni-Al layered double hydroxide (Ni-Al LDH) as an anode in nickel-metal hydride batteries is synthesized by liquid phase deposition (LPD) and the interlayer distance of the Ni-Al LDH is enlarged by the anionic exchanges from F^- form to halide anion forms, oxo anion forms, complex anion forms, and surface-active agent anion forms, namely, ca. from 320 pm to a maximum of 2500 pm. Then, we fabricate electrodes from the anion-exchanged LDH and study the relations between interlayer distance and internal resistance. The interlayer distances of the Ni-Al LDH, which are calculated from $d_{003,}$ increase with the diameter of the intercalated anions. The interlayer distance of the LDH depends

on the molecular shape and size of the intercalated anions. The charge transfer resistance(R_{ct}) decreases by half when the LDH interlayer distance increases to about 400 pm, and the activation energy for charge transfer(ΔE_a) also decreases with increasing LDH interlayer distance. Furthermore, the electron transfer and the ion transport between the collector (i.e., Ni foam) and the active material especially contribute to the decrease of R_{ct} and ΔE_a of the electrode compared with those between the conductive assistant (i.e., carbon black powder).

1. Introduction

The Ni-MH battery, with an aqueous electrolytic solution, is safer than the Li-ion battery, in which the electrolytic solution is inflammable organic solvent. Nickel hydroxide, $Ni(OH)_2$, which is one of the 3d transition metals, is important in the electrochemical field as electrode catalysts and electrode active materials [1-3], so various synthesis methods have been researched. The $Ni(OH)_2$ is generally applied to the positive electrode as a Ni-MH battery, and the charge/discharge reaction proceeds by the adsorption/desorption reaction of hydrogen in the hydrogen absorbing alloy, which is applied as a negative electrode as follows [4].

$$\text{Cathode; } Ni(II)(OH)_2 + OH^- \leftrightarrow Ni(III)OOH + H_2O + e^- \quad (1)$$

$$\text{Anode; } M + H_2O + e^- \leftrightarrow MH + OH^- \quad (2)$$

The nickel positive active material for the alkali storage battery used widely at present is β-$Ni(OH)_2$. β-$Ni(OH)_2$ is oxidized to β-NiOOH during the charging process and β-NiOOH is reduced to β-$Ni(OH)_2$ during the discharging process [5]. This redox reaction at the charge/discharge process is a one-electron transfer reaction, and the theoretical capacity is 289 mAh g^{-1}. A part of this β-NiOOH is changed to γ-NiOOH by the overcharge. γ-NiOOH has a well-developed layered structure, so the water molecules

and the K^+ ions in the electrolyte can be intercalated between the layers of the crystal lattice of γ-NiOOH. These intercalations increase the interlayer distance of γ-NiOOH, and bring about the volumetric change of electrodes and the concentration change of the electrolyte; consequently, there is a problem of these changes causing the degradation of battery characteristics, such as cycle characteristics. Hence, it has been considered that using γ-NiOOH for the charge/discharge cycle in the Ni-MH battery and increasing capacity through the contribution of γ-NiOOH are quite difficult, and moreover, Sato et al. has pointed out that the formation of the γ-NiOOH is one of the causes of the memory effect specific to a Ni-MH battery [6]. However, a part of nickel in γ-NiOOH is oxidized to quadrivalent [7-9], therefore, when γ-NiOOH functions as an active material for a positive electrode, the overall oxidation reaction in the charging process becomes a multi-electron reaction as follows.

$$\text{Cathode; } Ni(II)(OH)_2 + xOH^- \leftrightarrow Ni(II+x)O_2H_{2-x} + xH_2O + xe^- \quad (3)$$

where x theoretically shows maxima 1.67 [8]. Therefore, the capacity per unit weight of the active material will increase, and a drastic improvement of the battery capacity will be achieved [10]. α-$Ni(OH)_2$, which has α-phase crystalline structure, exists as a nickel hydroxide besides β-$Ni(OH)_2$. Advantageously, the difference in lattice constants between α-$Ni(OH)_2$ and γ-NiOOH is relatively small [4,10], and they have mutually similar crystal structures, hence the redox reaction progresses reversibly between α-$Ni(OH)_2$ and γ-NiOOH. Therefore, if this redox reaction is applied for a positive electrode reaction of a Ni-MH battery, the volumetric change during charge/discharge processes will be small, and the positive electrode capacity can be drastically improved [5,6]. However, α-$Ni(OH)_2$ is very chemically unstable in strongly alkaline solutions [10]; consequently, the novel synthetic procedure of the Ni-Al LDH, which substitutes a part of Ni^{2+} ions that form main frames in the LDH with Al^{3+} ions, has been proposed (Fig. S1) [10-23]. The LPD method enables a simple synthesis of nickel hydroxide

with the stable α-phase in strongly alkaline solutions by the introduction to main frames in the LDH of the trivalent cation, so the LDHs of high crystallinity and high purity can be synthesized by the LPD method [10,13,16,21,22,24,25]. In addition, the syntheses of various active materials to the surfaces on substrates of various materials that have complicate surface shapes, e.g., fine particles and the inner wall of small pores, are possible by the LPD method [10,15,24,26]. Therefore, we recently attempted the synthesis of Ni-Al LDH onto the surfaces of various conductive materials by using the LPD method. As a result, Ni-Al LDH coating onto the surface of carbon black powder, which is the conductive auxiliary for secondary battery electrodes, has been successful. In addition, the positive electrode for a Ni-MH battery was constructed by using this carbon black core Ni-Al LDH as an active material, and its electrochemical characteristic was evaluated [10,13,16,22,25]. This positive electrode showed excellent charge/discharge characteristics and the discharge capacity of 380 mAh g^{-1} was retained after 869 charge/discharge cycles [10]. However, because the adhesion among active materials and between current collectors and active materials in this positive electrode were poor, the causes of the charge transfer resistance were generated as follows: (1) contact resistance between current collector and active material, (2) charge transfer resistance between active material particles, and (3) charge transfer resistance in the active material particle interior.

Reducing the internal resistance of a battery is an important fundamental technology in developing secondary batteries [27-31]. It is obvious that the internal resistance causes the consequential battery power loss and the reduction of the battery internal resistance enables charge/discharge speed acceleration. To develop the positive electrode, which has high capacity and low charge transfer resistance, the direct synthesis of the Ni-Al LDH onto the surface of the electro conductive substrates by the LPD reaction has been carried out [32,33]. Because LPD can produce active material layers that are extremely adhered to the substrate, the charge transfer resistance between the current collector and active material drastically decreased when the current collector was used as the substrate. Enhancing the ion transport efficiency is also useful for a decrease in further internal

resistance. Therefore, in the present work, the interlayer distance of the Ni-Al LDH was increased by the intercalation into the LDH interlayer of the anions, which have various ionic radii. Furthermore, we investigated how the electrode influenced the internal resistance by examining the interlayer distance of the Ni–Al LDH, using the LDH sample as the active material. Moreover, to clarify the effect to the ion transport by the enlargement of LDH interlayer distance, the activation energy (ΔE_a) of the anion exchanged Ni–Al LDH electrodes was evaluated with electrochemical impedance spectroscopy (EIS).

2. Experimental section

2.1. Preparation of Ni-Al LDH by the LPD Reaction

All chemicals used in this work were of analytical grade. The Ni-Al LDH was prepared by the LPD reaction as shown in Scheme S1. Commercially available β-$Ni(OH)_2$, obtained from dehydration purification, is hard to dissolve even in acidic conditions. Hence, in this study β-$Ni(OH)_2$ was synthesized by hydrolyzing the nickel ion. About 15% NH_3 aq. was added into 0.4 mol L^{-1} $Ni(NO_3)_2$ aq. until pH 7.5 under stirring, and to remove NO_3^- anion, precipitated β-$Ni(OH)_2$ was filtered off by suction filtration. 0.5 mol L^{-1} HF was added until the β-$Ni(OH)_2$ dissolved as a nickel fluoride complex in a plastic flask. Then, 15% ammonia water was added in dropwise fashion until pH 7.5, and the total volume was adjusted to 1 L. The total Ni^{2+} ion concentration was 12 mmol L^{-1}, and the total F^- ion concentration and pH of an appropriate amount of the solution were adjusted by adding hydrofluoric acid and NH_3 aq. to 200 mmol L^{-1} and 8.2, respectively. Then, the total Al^{3+} concentration in the LPD reaction solution was adjusted to 2 mmol L^{-1} by $Al(NO_3)_3$ aq. In this study, the concentration of Ni^{2+} ion should be lower than that in our previous report [10] because of the elution of Ni^{2+} ion from the Ni foam substrate. Proper amount of carbon black powder (CB; 3050B, Mitsubishi Chemical Corp., Japan) or foam nickel plate (Ni foam; Celmet #8, Sumitomo Electric Industries, Ltd., Japan), which apply the surface hydrophilization by ozone oxidation using an ozone/UV surface treatment system (EKBIO-

1100, Ebara Jitsugyo Co. Ltd., Japan), were added as a substrates into the proper amount of LPD reaction solution, and reacted at 50 °C for 48 h. Finally, the substrates were washed and dried at room temperature.

2.2. Anion exchange of as-deposited Ni-Al LDH

A proper amount of the prepared Ni-Al LDH (as-dep. LDH) was added into aqueous solutions of various anions, that is, 1 mol L^{-1} KCl, KBr, KI, KNO_3, K_2CO_3, $ZnSO_4$, 0.1 mol L^{-1} $K_4[Fe(CN)_6]$, 5 mmol L^{-1} sodium dodecyl sulfate (SDS), or 1 mmol L^{-1} sodium dodecyl benzene sulfonate (DBS) aq. Both these concentrations of SDS and DBS, which are the surface active agents, are below the critical micelle concentration. The anion exchange reaction in the interlayer of the as-dep. Ni-Al LDH samples was carried out under stirring for 24 h. The as-dep. and anion exchanged Ni-Al LDH thin films were characterized by an X-ray diffractometer (XRD; RINT-TTR/S2, Rigaku Corp., Japan), an inductively coupled plasma atomic emission spectrometry (ICP-OES; ULTIMA 2000, HORIBA Ltd., Japan), and a field emission scanning electron microscope (FE-SEM; JEM-6335F, JEOL Ltd., Japan). An EDX elemental mapping analyzer (EDX; EX-23000BU, JEOL Ltd., Japan) of the FE-SEM was used to elucidate the distribution of Ni and Al. The anion exchange rate from the as-dep. Ni–Al LDH was determined by ion chromatography (JASCO, Japan).

2.3. Assembling of electrochemical cell and electrochemical measurements

The positive electrode of an electrochemical cell was prepared as follows(see also Scheme S2): 5.0 mg of anion exchanged CB core LDH powder, which contains anion exchanged Ni-Al LDH of 71.0 wt% (LDH/CB), was mixed with 20 mg of 2 g cm^{-3} polyvinyl alcohol (PVA) aq. as a binder to make a paste. The resulting paste was loaded onto a 1 × 1.5 cm^2 anion exchanged LDH on Ni foam (LDH/Ni foam), and dried under vacuum at 80 °C for 1 h, then pressed at 20 MPa for 1 min. The Hg/HgO into 6 mol L^{-1} KOH aq. and the Ni foam were employed as the reference electrode and the counter electrode,

respectively, while 6 mol L^{-1} KOH aq. served as an electrolyte solution. All electrochemical measurements were performed using VoltaLab (Radiometer Analytical S.A., PGZ402, France) at 25 °C. The cyclic voltammetry (CV) experiments were carried out in the potential region of 0–600 mV vs. Hg/HgO at a scan rate of 1 mV s^{-1} for 10 repeated cycles. After CV measurement, to clarify the interlayer distance dependence on the charge transfer resistance of the electrodes, the EIS experiments were operated on Voltalab at 25 °C and the potential condition of 500 mV vs. Hg/HgO as the reference electrode after 10 repeated cycles of CV. The EIS data were collected as a function of frequency scanned from 10 kHz to 50 mHz, and the amplitude of the perturbation voltage was set at 5 mV.

3. Results and discussion

3.1. Anion exchange of the Ni–Al LDH prepared by LPD

Fig. 1(a) and (b) shows the surface morphologies, by SEM micrograph, and the corresponding EDX spectra in the Ni–Al LDH thin films on the surfaces of Ni foam (Fig. 1(a)) and carbon black powder (Fig. 1(b)) without anion exchange. The composition formulas and the thickness of the Ni–Al LDH thin films on the surfaces of Ni foam and carbon black powder without anion exchange, which were determined from the ICP-OES and the cross-sectional FE-SEM measurements, were $Ni_{0.95}Al_{0.05}(OH)_2F_{0.05}$ and $Ni_{0.76}Al_{0.24}(OH)_2F_{0.24}$, and 460 nm and 900 nm, respectively. These measurements revealed an adequate amount and uniform distribution of Al^{3+} in the Ni-Al LDH and verified that Al^{3+} ions were introduced into the LDH main frame. The introduction of trivalent cations, such as Al^{3+}, into the LDH main frame will help to stabilize the α-phase of nickel hydroxide and to improve the material's electrochemical properties [13,16]. The SEM images reveal that many densely packed, regular plate-like particles of Ni–Al LDHs formed, a result that does not depend on the substrate material or shape. Moreover, the width of the XRD signals of the (003) plane of the Ni–Al LDH did not depend on the substrate material, revealing that the crystallinity of the LDH prepared by LPD was not affected by the substrate material. In our previous work, we observed that direct anion

exchange of Ni–Al LDH for OH^-–, Cl^-–, SO_4^{2-}–, and CH_3COO^- maintained high crystallinity and increased the interlayer distance [24]. In the case of Cl^- form Ni-Al LDH, the anion exchange rate was 89%, that is, the composition formulas of the Ni-Al LDH thin films on the surfaces of Ni foam and carbon black powder with anion exchange were $Ni_{0.95}Al_{0.05}(OH)_2Cl_{0.03}F_{0.02}$ and $Ni_{0.76}Al_{0.24}(OH)_2Cl_{0.14}F_{0.10}$, respectively.

Fig. 2 shows the difference between the increases in the crystal face spacing d_{003} using XRD measurements of the LDH by direct and indirect anion exchange treatment (i.e., one-step and two-step anion exchange). The d_{003} values were calculated from the XRD signal of the (003) plane using Bragg's equation. In the case of the anions whose molecular size is greater than 900 pm—namely, $[Fe(CN)_6]^{4-}$ as the complex anion, dodecyl sulfate anion (i.e., DS^-) and dodecyl benzene sulfonate anion (i.e., BS^-) as the surface-active agent anions—the anions had not been intercalated into the interlayer of the as-deposited LDH by the one-step anion exchange treatment because their ionic size is too large, as shown in Fig. 2(a). Conversely, the d_{003} values of the two-step anion exchange (i.e., the preliminary interlayer distance expansion by SO_4^{2-} anion) treated LDH increased from 779 pm to 1091 pm, as shown in Fig. 2(b), and similar results were also confirmed for DS^- and BS^- anions. Therefore, these large anions have been intercalated by the two-step anion exchange treatment.

3.2. Relationship between LDH interlayer distance and molecular size of intercalated anions

Fig. 3 shows the correlation between the interlayer distance of the anion exchanged Ni-Al LDH thin films on a Ni foam surface and the molecular size of the anions intercalated in the LDH interlayer. The interlayer distances were calculated by the following equation from the d_{003} values, which were determined by XRD.

$$\text{Interlayer distance} = d_{003} - \text{Ni-Al LDH layer thickness} \quad (3)$$

where the Ni-Al LDH layer thickness is 460 pm as our previous report, and the diameters of the anions were referred from previous reports [34]. The diameters of the anions come from previous reports [35-38]. The Ni-Al LDH interlayer distance increased simply with the molecular size of the intercalated anions. However, it should be noted that the interlayer distance did not increase linearly with increasing molecular size. When the molecular size of the intercalated anions was less than about 380 pm, which is the diameter of a water molecule, the LDH interlayer distance hardly changed because of the intercalation of water molecules. Essentially, this behavior occurred because the water molecules greatly influenced the LDH interlayer. Moreover, the LDH interlayer distance also hardly changed with the intercalation of DS^- and BS^- anions. This suggested that BS^-, which has a high molecular length (i.e., 2260 pm), is intercalated in the inclined state against the LDH interlayer plane compared with DS^-, whose molecular length is shorter than BS^- (i.e., 1360 pm).

Fig. 4 shows the surface morphology change observed by SEM micrograph, with the interlayer distance of anion exchanged Ni-Al LDH thin film on Ni foam surface. Regardless of the difference of substrate material, many regular plate-like particles of LDHs formed densely on the surface in these SEM images of the LDH without anion exchange. The overall LDH layered structure swelled with the increase in the interlayer distance by the anion exchange to SO_4^{2-} and $[Fe(CN)_6]^{4-}$ forms. Finally, the peculiar LDH network structure disappeared and changed into an agglomerated particle structure by intercalation of DS^- anion. A new ionic conduction path might have been constructed in the Ni-Al LDH by these structure changes. Therefore, these changes in the interlayer distance and the surface structure of the Ni-Al LDH may improve the charge-discharge behavior of nickel-hydrogen batteries by improving the charge-transfer and ion-transport properties of the active material.

3.3. Charge-transfer properties of electrodes fabricated by anion-exchanged Ni-Al LDH

Based on the above discussion, the charge transfer resistance, R_{ct}, of the electrode fabricated using anion-exchanged Ni-Al LDH was determined by EIS (i.e., electrochemical impedance

spectroscopy) measurement, so as to investigate how increasing the Ni-Al LDH interlayer distance affected the charge transfer properties. Figs. S2-S4 show the Nyquist plots of Ni-Al LDH thin films anion-exchanged with various halide anions (Figs. S2-S4(a)) and oxoanions, complex anions, and surface-active agent anions (Figs. S2-S4(b)). Anion exchange was performed for the Ni-Al LDH thin films on the surface of both Ni foam and/or carbon black powder (i.e., the surfaces of both Ni foam and carbon black powder (Fig. S2), the surface of Ni foam only (Fig. S3), and the surface of carbon black powder only (Fig. S4)). The R_{ct} was determined from the diameter of the semicircle in the Nyquist plot by a transmission line model that considered charge transfer resistance and electrochemical reaction [39], as shown in Fig. S2(a).

CV of the Ni−Al LDH thin film which was anion exchanged by $[Fe(CN)_6]^{4-}$ anion is shown in Fig. S5. No peak related to the redox reaction of $[Fe(CN)_6]^{4-}$ anion is confirmed. This shows that $[Fe(CN)_6]^{4-}$ anion is hardly exist between the Ni-Al LDH layers, because the redox reaction in the cathode almost proceed in the Ni-Al LDH existing near the electrode surface. The $[Fe(CN)_6]^{4-}$ anion which extended the Ni-Al LDH interlayer distance by the ion exchange from the SO_4^{2-} anion exudes into the electrolytic solution from the Ni-Al LDH interlayer by the ion exchange with the OH^- anions in the electrolytic solution (i.e., 6 mol L^{-1} KOH aq.).

Fig. 5 shows the interlayer distance dependence of the R_{ct} of the anion-exchanged Ni-Al LDH on the surfaces of both the Ni foam and carbon black powder. It is noteworthy that the R_{ct} obviously decreased as the interlayer distance increased. This shows that the ion transport and the electron transfer became smooth because of the expansion of the LDH interlayer distance. Furthermore, the R_{ct} decrease was caused by the extension of a small interlayer distance of the layered double hydroxide from 320 (i.e., F^- form) to 370 nm (i.e., SO_4^{2-} form). In addition, to clarify the effective contribution of the electrode to reducing the charge transfer resistance, two more kinds of electrodes were prepared and their EIS were measured: first, the LDH with anion exchange on the Ni foam surface combined with the LDH without anion exchange on the carbon-black powder surface (i.e., CC electrode), and second, the

LDH without anion exchange on the Ni foam surface combined with the LDH with anion exchange on the carbon-black powder surface (i.e., CA electrode). Thus, the electrode used in Fig. 5 can be presented as a CC+CA electrode.

Fig. 6 shows the influence on anion exchange part to the interlayer distance dependence on R_{ct} of the anion-exchanged Ni-Al LDH on the surfaces of the Ni foam and/or carbon black powder. The R_{ct} values of the CA electrode without anion exchange for the LDH on the Ni foam surface is clearly large. In contrast, the CC and CA+CC electrodes with anion exchange for the LDH on the Ni foam surface have small R_{ct}. This clearly shows that the electron transfer and the ion transport between the collector and the active material especially contributes to a decrease of the R_{ct}. Fig. 7 shows the influence on anion exchange part to the interlayer distance dependence on the apparent activation energies, ΔE_a, of the charge transfer in the anion-exchanged Ni-Al LDH on the surfaces of the Ni foam and/or carbon black powder. The ΔE_a values were determined using the Arrhenius plots, which is the temperature dependence on the reciprocal of the charge-transfer resistance as shown in Fig. S6. According to our previous report, the ΔE_a of the electrode without any anion exchange for the Ni-Al LDH on the surfaces of both the Ni foam and carbon black powder was 21.8 kJ mol^{-1} [33]. The ΔE_a obtained in this work obviously decreased with increasing LDH interlayer distance. Moreover, the ΔE_a of the CC and CA+CC electrodes were much smaller than that of the CA electrode, as well as for the R_{ct}. These R_{ct} and ΔE_a results show the ion transport and the electron transfer became smooth because of the expansion of the LDH interlayer distance. Additionally, the improvements in the ion transport and the electron transfer in the interface between the collector and the active material especially contribute to a decrease in the internal resistance of an electrode. Incidentally, the anion exchanged Ni-Al LDH is immersed in 6 mol L^{-1} KOH aq. during the electrochemical measurement; hence, there is a possibility that the anion of the LDH interlayer was exchanged for the OH^- ion. Consequently, the OH^- quantities in the interlayer of anion-exchanged Ni-Al LDHs were determined by pH titration as shown in Fig. S7.

The OH^- quantity in the LDH interlayer obviously decreases according to the increase in the interlayer distance, and this trend is remarkable for DS^- and BS^-. It is expected that the regularity of the LDH layered structure decreases because of a remarkable increase in the interlayer distance. Therefore, it can be concluded that the main factor for decreasing R_{ct} is not the OH^- anions in the LDH interlayer but the interlayer distance. The results obtained in this research are useful for the development of secondary batteries that have low internal resistance and high-speed charge/discharge properties.

4. Conclusions

The Ni-Al LDH has been synthesized on the Ni foam surface and the carbon black powder surface by the LPD procedure. The adequate amount and uniform distribution of Al^{3+} in the Ni-Al LDH main frame has been revealed. The F^- ion in the as-deposited Ni-Al LDH interlayer has been exchanged by the ion-exchange reaction to the anions, which have various ionic radii such as halide anion forms, oxo anion forms, complex anion forms, and surface-active agent anion forms. In the case of anions with a molecular size greater than 900 pm, namely $[Fe(CN)_6]^{4-}$, DS^- and BS^-, these anions have been intercalated into the interlayer of the as-deposited LDH by the two-step anion exchange by the preliminary interlayer distance expansion using SO_4^{2-} anions. As a result, the interlayer distance of the Ni-Al LDH has been enlarged from 320 pm (F^- form) to a maximum of about 2500 pm (BS^- form) by these anionic exchanges. The peculiar LDH network structure disappeared and changed into an agglomerated particle structure by intercalation of surface-active agent anion, and a new ionic conduction path has been constructed in the Ni-Al LDH by these structure changes. The R_{ct} and the ΔE_a of charge transfer of anion-exchanged Ni-Al LDH on the surfaces of both Ni foam and carbon black powder obviously decreased as the interlayer distance increased, and the R_{ct} and ΔE_a decrease was caused by the extension of a small interlayer distance of the layered double hydroxide from 320 (i.e., F^- form) to 370 nm (i.e., SO_4^{2-} form). Furthermore, the electron transfer and the ion transport between the collector (i.e., Ni foam) and the active material especially contribute to the decrease of R_{ct} and ΔE_a of

the electrode compared with those between the conductive assistant (i.e., carbon black powder). The results obtained in this research are useful for the development of the secondary batteries that have low internal resistance and high-speed charge/discharge properties.

Acknowledgment

This study was carried out under the Technology Development of Energy Storage System for Grid Stabilization Projects; "Development of Safety and Cost Competitive Energy Storage System for Renewable Energy" (No. 12101435-0) supported by Kawasaki Heavy Industries, Ltd. and New Energy and Industrial Technology Development Organization (NEDO).

References

[1] H. Inoue, Y. Namba, E. Higuchi, Preparation and characterization of Ni-based positive electrodes for use in aqueous electrochemical capacitors, J. Power Sources 195 (2010) 6239–6244.

[2] K. Nishimura, T. Takasaki, T. Sakai, Introduction of large-sized nickel–metal hydride battery GIGACELL® for industrial applications, J. Alloys Compd. 580 (2013) S353–S358.

[3] T. Takasaki, K. Nishimura, M. Saito, H. Fukunaga, T. Iwaki, T. Sakai, Cobalt-free nickel–metal hydride battery for industrial applications, J. Alloys Compd. 580 (2013) S378–S381.

[4] H. Bode, K. Dehmelt, J. Witte, Zur kenntnis der nickelhydroxidelektrode—I.Über das nickel (II)-hydroxidhydrat, Electrochim. Acta 11 (1966) 1079−1087.

[5] A. Delahaye-Vidal, M. Figlarz, Textural and structural studies on nickel hydroxide electrodes. II. Turbostratic nickel (II) hydroxide submitted to electrochemical redox cycling, J. Appl. Electrochem. 17 (1987) 589−599.

[6] M. Morishita, Y. Shimizu, K. Kobayakawa, Y. Sato, Suppression of the memory effect observed in alkaline secondary batteries under partial charge–discharge conditions, Electrochim. Acta 53 (2008) 6651−6656.

[7] P. Oliva, J. Leonardi, J.F. Laurent, C. Delmas, J.J. Braconnier, M. Figlarz, F. Fievet, A.de Guibert, Review of the structure and the electrochemistry of nickel hydroxides and oxy-hydroxides, J. Power Sources 8 (1982) 229−255.

[8] D. A. Corrigan, S. L. Knight, Electrochemical and Spectroscopic Evidence on the Participation of Quadrivalent Nickel in the Nickel Hydroxide Redox Reaction, J. Electrochem. Soc. 136 (1989) 613−619.

[9] A. Van der Ven, D. Morgan, Y. S. Meng, G. Ceder, Phase Stability of Nickel Hydroxides and Oxyhydroxides, J. Electrochem. Soc. 153 (2006) A210−A215.

[10] A. B. Béléké, E. Higuchi, H. Inoue, M. Mizuhata, Durability of nickel–metal hydride (Ni–MH) battery cathode using nickel–aluminum layered double hydroxide/carbon (Ni–Al LDH/C) composite, J. Power Sources 247 (2014) 572−578.

[11] B. Eang, Q. Liu, Z. Qian, X. Zhang, J. Wang, Z. Li, H. Yan, Z. Gao, F. Zhao, L. Liu, Two steps in situ structure fabrication of Ni–Al layered double hydroxide on Ni foam and its electrochemical performance for supercapacitors, J. Power Sources 246 (2014) 747−753.

[12] L. J. Zhang, L. Zhang, D. Tao, X. Huang, Enhanced high-current capacitive behavior of graphene/CoAl-layered double hydroxide composites as electrode material for supercapacitors, J. Power Sources 199 (2012) 395−401.

[13] A. B. Béléké, E. Higuchi, H. Inoue, M. Mizuhata, Effects of the composition on the properties of nickel–aluminum layered double hydroxide/carbon (Ni–Al LDH/C) composite fabricated by liquid phase deposition (LPD), J. Power Sources 225 (2013) 215−220.

[14] L. X. Xie, Z. Hu, C. Lv, G. Sun, J. Wang, Y. Li, H. He, J. Wang, K. Li, Co_xNi_{1-x} double hydroxide nanoparticles with ultrahigh specific capacitances as supercapacitor electrode materials, Electrochim. Acta 78 (2012) 205−211.

[15] H. Maki, Y. Okumura, H. Ikuta, M. Mizuhata, Ionic Equilibria for Synthesis of TiO_2 Thin Films by the Liquid-Phase Deposition, J. Phys. Chem. C 118 (2014) 11964−11974.

[16] A. B. Béléké, M. Mizuhata, Electrochemical properties of nickel–aluminum layered double hydroxide/carbon composite fabricated by liquid phase deposition, J. Power Sources 195 (2010) 7669−7676.

[17] A. Sugimoto, S. Ishida, K. Hanawa, Preparation and Characterization of Ni/Al‐Layered Double Hydroxide, J. Electrochem. Soc. 146 (1999) 1251−1255.

[18] Z. Gao, J. Wang, Z. Li, W. Yang, B. Wang, M. Hou, Y. He, Q. Liu, T. Mann, P. Yang, M. Zhang, L. Liu, Graphene Nanosheet/Ni^{2+}/Al^{3+} Layered Double-Hydroxide Composite as a Novel Electrode for a Supercapacitor, Chem. Mater. 23 (2011) 3509−3516.

[19] Y. Wang, D. Zhang, W. Peng, L. Liu, M. Li, Electrocatalytic oxidation of methanol at Ni–Al layered double hydroxide film modified electrode in alkaline medium, Electrochim. Acta 56 (2011) 5754−5758.

[20] P. V. Kamath, M. Dixit, L. Indira, A. K. Shukla, Y. G. Kumar, N. Munichandraiah, Stabilized α-$Ni(OH)_2$ as Electrode Material for Alkaline Secondary Cells, J. Electrochem. Soc. 141 (1994) 2956−2959.

[21] Q. Liu, G. Fan, S. Zhang, Y. Liu, F. Li, Synthesis of uniform Ni–Al layered double hydroxide via a novel reduction–oxidation route, Mater. Lett. 82 (2012) 4−6.

[22] M. Mizuhata, A. Hosokawa, A. B. Béléké, S. Deki, Ni–Al Layered Double Hydroxide Prepared by Liquid Phase Deposition, Chem. Lett. 38 (2009) 972−973.

[23] M. Morishita, T. Kakeya, S. Ochiai, T. Ozaki, Y. Kawabe, M. Watabe, T. Sakai, Structural analysis by synchrotron X-ray diffraction, X-ray absorption fine structure and transmission electron microscopy for aluminum-substituted α-type nickel hydroxide electrode, J. Power Sources 193 (2009) 871−877.

[24] H. Maki, Y. Mori, Y. Okumura, M. Mizuhata, Anion-exchange properties of nickel–aluminum layered double hydroxide prepared by liquid phase deposition. Mater. Chem. Phys. 141 (2013) 445−453.

[25] A. B. Béléké, A. Hosokawa, M. Mizuhata, S. Deki, Preparation of α-nickel hydroxide/carbon composite by the liquid phase deposition method, J. Ceram. Soc. Jpn. 117 (2009) 392−394.

[26] Y. Aoi, H. Kambayashi, T. Deguchi, K. Yato, S. Deki, Synthesis of nanostructured metal oxide by liquid-phase deposition, Electrochim. Acta 53 (2007) 175−178.

[27] S. –K. Chen, K. –F. Chiu, S. –H. Su, S. –H. Liu, K. H. Hou, H. –J. Leu, C. –C. Hsiao, Low contact resistance carbon thin film modified current collectors for lithium Ion batteries, Thin Solid Films 572 (2014) 56−60.

[28] H. –C. Wu, H. –C. Wu, E. Lee, N. –L. Wu, High-temperature carbon-coated aluminum current collector for enhanced power performance of $LiFePO_4$ electrode of Li-ion batteries, Electrochem. Commun. 12 (2010) 488−491.

[29] B. Jeong, S. Uhm, J. –H. Kim, J. Lee, Pyrolytic carbon infiltrated nanoporous alumina reducing contact resistance of aluminum/carbon interface, Electrochim. Acta 89 (2013) 173−179.

[30] E. Taer, M. Deraman, I. A. Talib, S. A. Hashmi, A. A. Umar, Growth of platinum nanoparticles on stainless steel 316L current collectors to improve carbon-based supercapacitor performance, Electrochim. Acta 56 (2011) 10217−10222.

[31] C. Lei, F. Markoulidis, Z. Ashitaka, C. Lekakou, Reduction of porous carbon/Al contact resistance for an electric double-layer capacitor (EDLC), Electrochim. Acta 92 (2013) 183−187.

[32] H. Maki, M.Takigawa, M. Mizuhata, Nickel–Aluminum Layered Double Hydroxide Coating on the Surface of Conductive Substrates by Liquid Phase Deposition, ACS Appl. Mater. Interfaces 7 (2015) 17188−17198.

[33] M. Takigawa, H. Maki, M. Mizuhata, Coating Current Collector Surface with Ni–Al Layered Double Hydroxide by Liquid Phase Deposition to Reduce Charge-Transfer Resistance, Electrochemistry 83 (2015) 803−806.

[34] X. Wang, H. Luo, P. V. Parkhutik, A. Millan, E. Matveeva, Studies of the performance of nanostructural multiphase nickel hydroxide, J. Power Sources 115 (2003) 153−160.

[35] R. D. Shannon, Revised effective ionic radii and systematic studies of interatomic distances in halides and chalcogenides, Acta Cryst. A32 (1976) 751−767.

[36] Y. Marcus, Ionic Liquid Properties, Springer International Publishing, New York, 2016, p. 21−22.

[37] M. Sammalkorpi, M. Karttunen, M. Haataja, Ionic Surfactant Aggregates in Saline Solutions: Sodium Dodecyl Sulfate (SDS) in the Presence of Excess Sodium Chloride (NaCl) or Calcium Chloride ($CaCl_2$), J. Phys. Chem. B 113 (2009) 5863−5870.

[38] K. Yang, L. Zhu, B. Xing, Sorption of sodium dodecylbenzene sulfonate by montmorillonite, Environ. Pollut. 145 (2007) 571−576.

[39] Z. Shiroma T. Ioroi, Expected Electrochemical Impedance Responses of Porous Electrodes Based on Theoretical Solutions of Transmission-line Models, Electrochemistry 83 (2015) 425−433.

Figure captions

Fig. 1. Surface morphologies by SEM micrographs and corresponding EDX spectra of the Ni−Al LDH thin films on the surfaces of Ni foam (a) and carbon black powder (b) deposited by the LPD reaction at 50 °C for 48 h, and X-ray diffraction patterns of Ni−Al LDH thin films on the surface of various substrates (c). The EDX spectrum for nickel element about the Ni-Al LDH thin films on the surfaces of Ni foam substrate was not measured. The concentrations of Ni^{2+} and Al^{3+} in the LPD reaction solution were 12 mmol L^{-1} and 2.0 mmol L^{-1}, respectively, and the total concentration of fluorine is 200 mmol L^{-1}.

Fig. 2. Difference between the increases in the crystal face spacing, d_{003}, using XRD measurements of the LDH by the one-step and two-step anion exchange. (a) One step direct anion exchange, (b) Two step indirect anion exchange. The d_{003} values were calculated from the XRD signal of the (003) plane using Bragg's equation.

Fig. 3. Anion diameter dependence of the interlayer distance of the anion exchanged Ni-Al LDH thin films on a Ni foam surface. The anion diameters for DS^- and BS^- anions show the molecular length of these anions.

Fig. 4. Surface morphology change observed by SEM micrograph with the interlayer distance of anion exchanged Ni−Al LDH thin film on Ni foam surface.

Fig. 5. Ni-Al LDH interlayer distance dependence on the charge transfer resistance of the electrode whose active material is the anion exchanged Ni-Al LDH. The anion exchange was carried out for Ni-Al LDH thin films on the surfaces of both Ni foam and carbon black powder.

Fig. 6. Influence on anion exchange part to the Ni-Al LDH interlayer distance dependence on the charge transfer resistance of the electrode whose active material is the anion exchanged Ni-Al LDH. The anion exchange was carried out for Ni-Al LDH thin films on the surfaces of Ni foam and/or carbon black powder.

Fig. 7. Influence on anion exchange part to the Ni-Al LDH interlayer distance dependence on the apparent activation energies of the charge transfer of the electrode whose active material is the anion exchanged Ni-Al LDH. The apparent activation energies were determined using the Arrhenius equation.

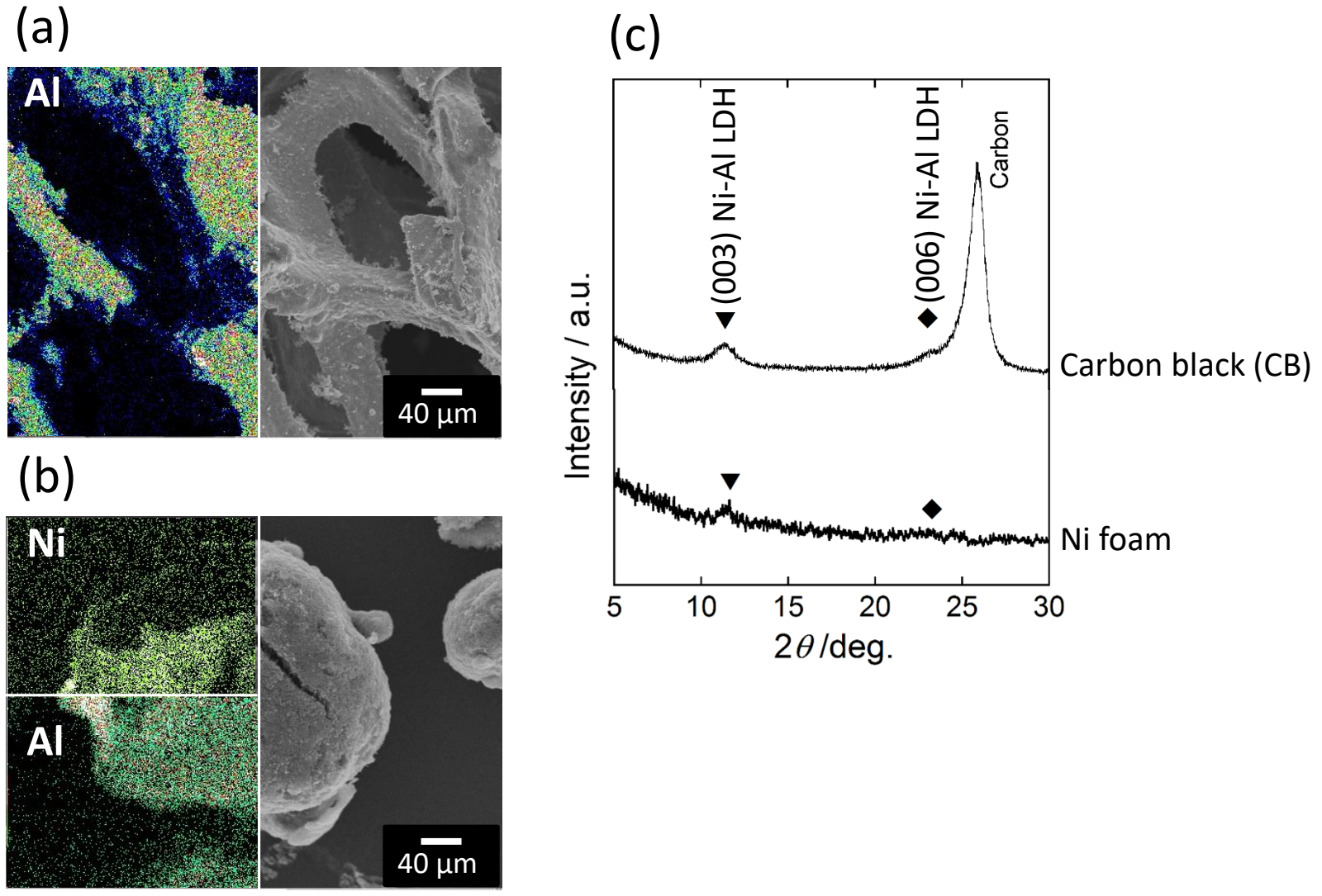

Fig. 1. Surface morphologies by SEM micrographs and corresponding EDX spectra of the Ni−Al LDH thin films on the surfaces of Ni foam (a) and carbon black powder (b) deposited by the LPD reaction at 50 ° C for 48 h, and X-ray diffraction patterns of Ni−Al LDH thin films on the surface of various substrates (c). The EDX spectrum for nickel element about the Ni-Al LDH thin films on the surfaces of Ni foam substrate was not measured. The concentrations of Ni^{2+} and Al^{3+} in the LPD reaction solution were 12 mmol L^{-1} and 2.0 mmol L^{-1}, respectively, and the total concentration of fluorine is 200 mmol L^{-1}.

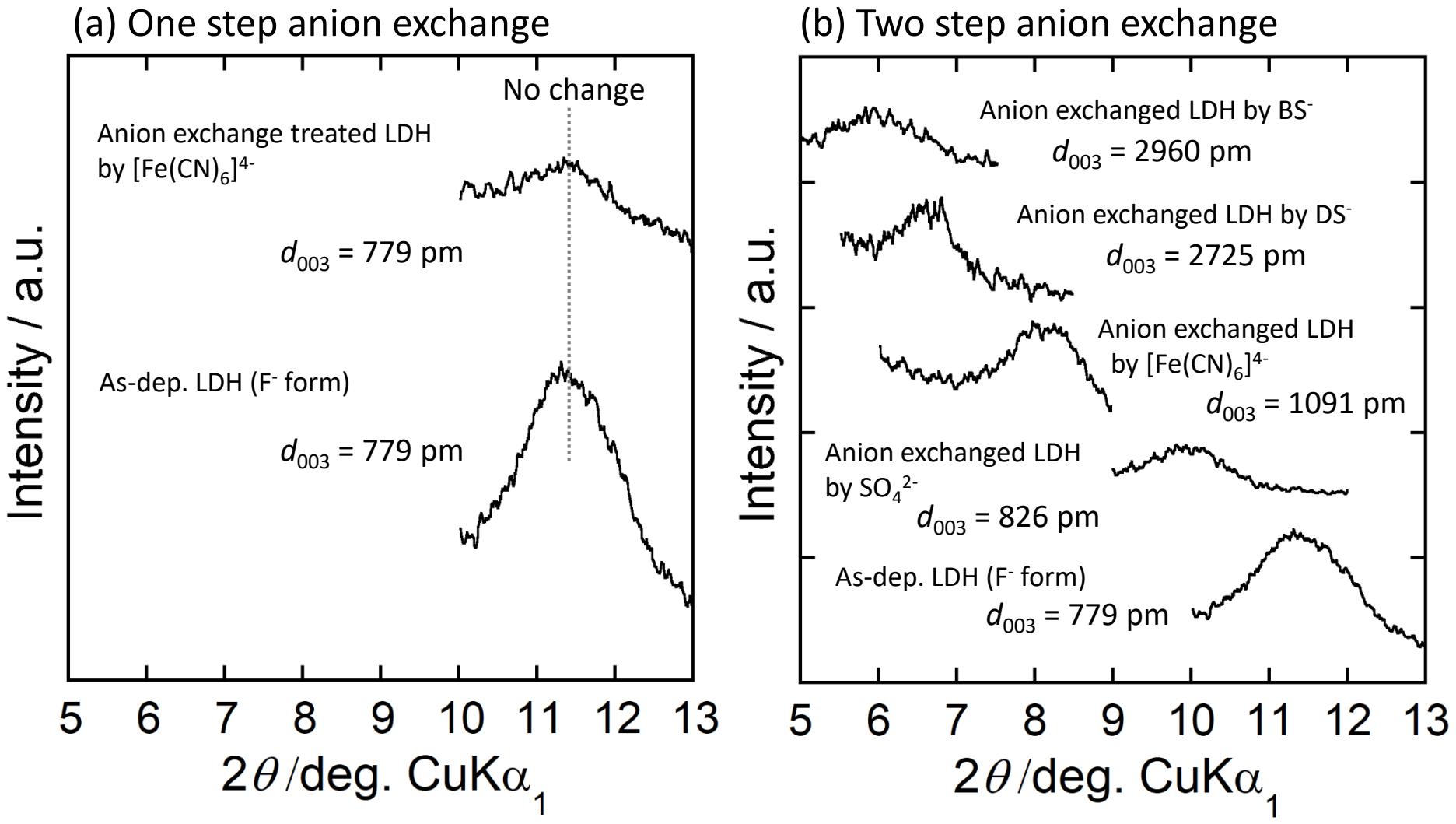

Fig. 2. Difference between the increases in the crystal face spacing, d_{003}, using XRD measurements of the LDH by the one-step and two-step anion exchange. (a) One step direct anion exchange, (b) Two step indirect anion exchange. The d_{003} values were calculated from the XRD signal of the (003) plane using Bragg's equation.

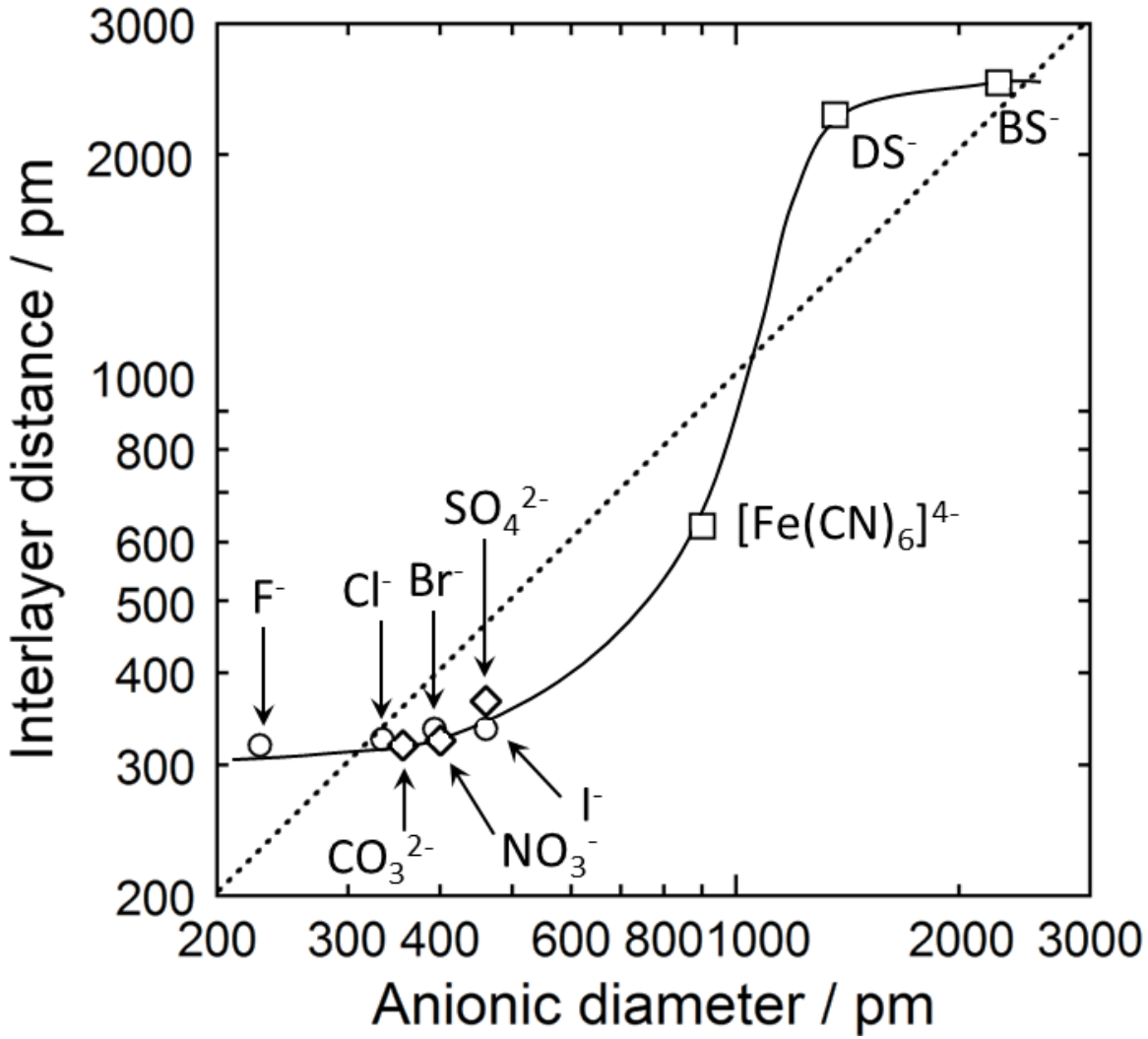

Fig. 3. Anion diameter dependence of the interlayer distance of the anion exchanged Ni-Al LDH thin films on a Ni foam surface. The anion diameters for DS^- and BS^- anions show the molecular length of these anions.

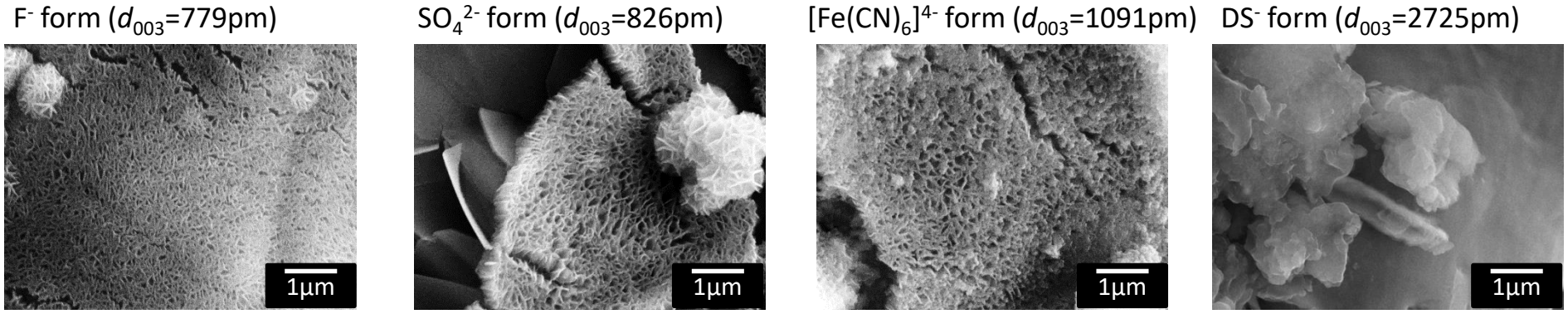

Fig. 4. Surface morphology change observed by SEM micrograph with the interlayer distance of anion exchanged Ni−Al LDH thin film on Ni foam surface.

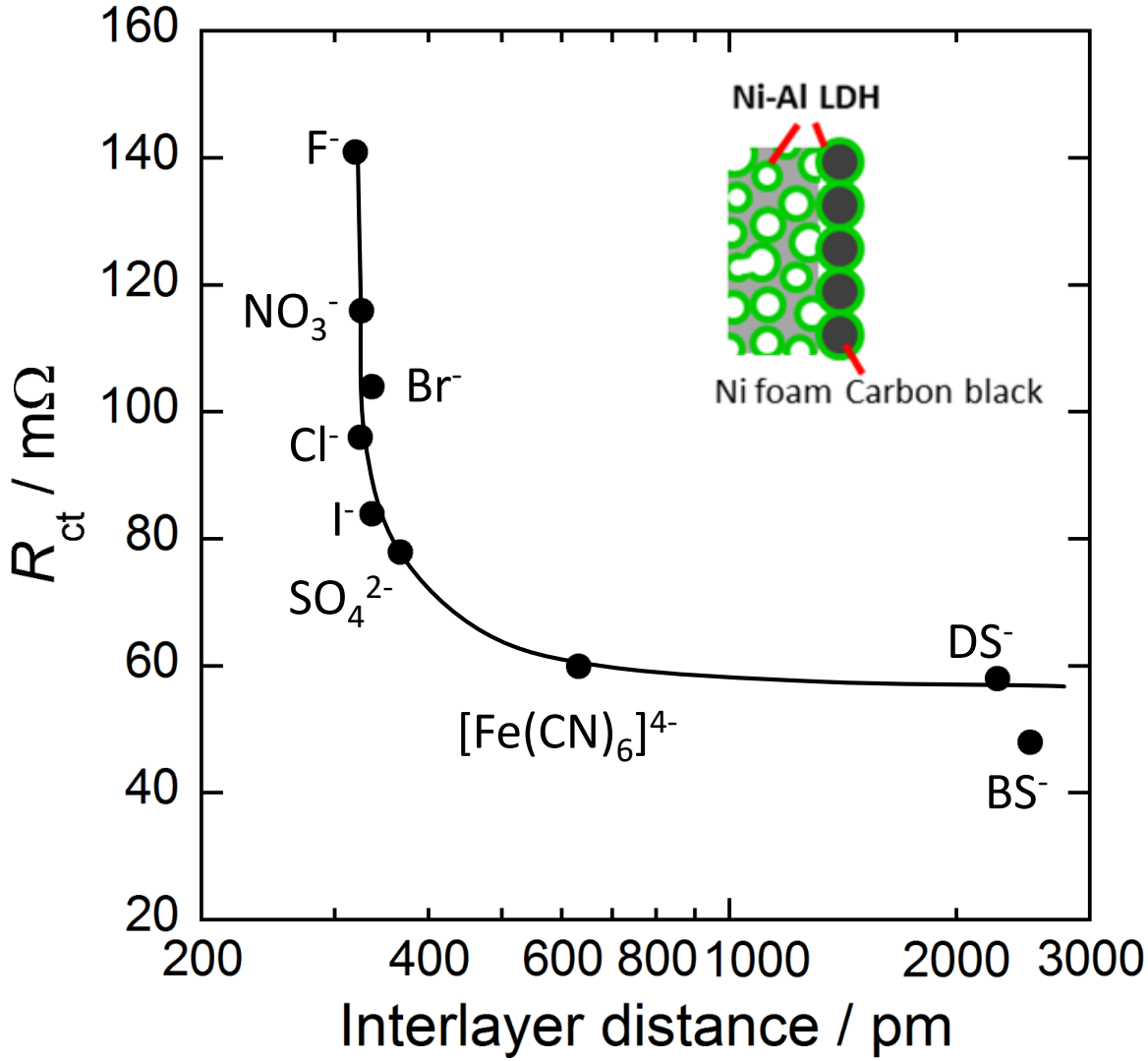

Fig. 5. Ni-Al LDH interlayer distance dependence on the charge transfer resistance of the electrode whose active material is the anion exchanged Ni-Al LDH. The anion exchange was carried out for Ni-Al LDH thin films on the surfaces of both Ni foam and carbon black powder.

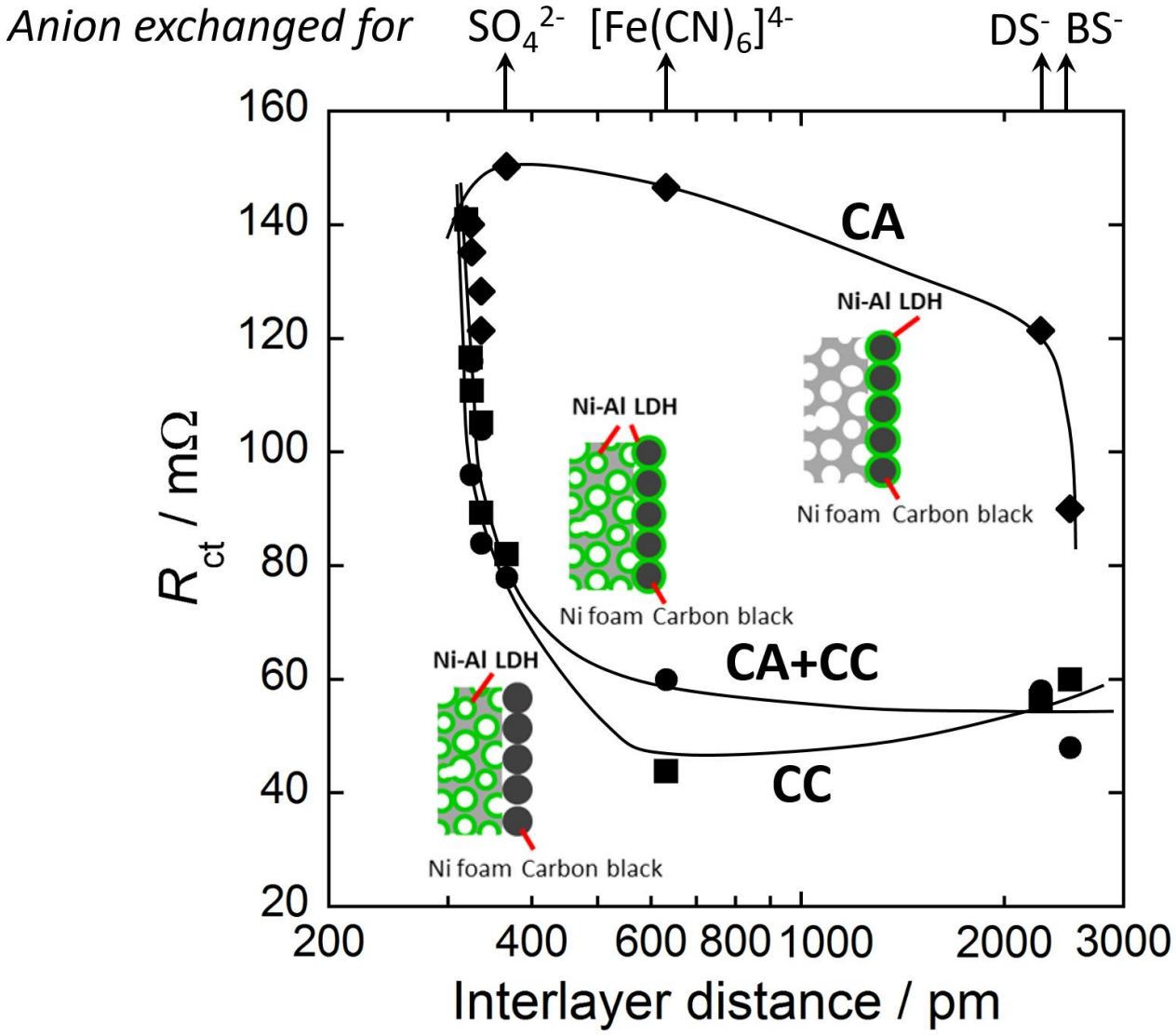

Fig. 6. Influence on anion exchange part to the Ni-Al LDH interlayer distance dependence on the charge transfer resistance of the electrode whose active material is the anion exchanged Ni-Al LDH. The anion exchange was carried out for Ni-Al LDH thin films on the surfaces of Ni foam and/or carbon black powder.

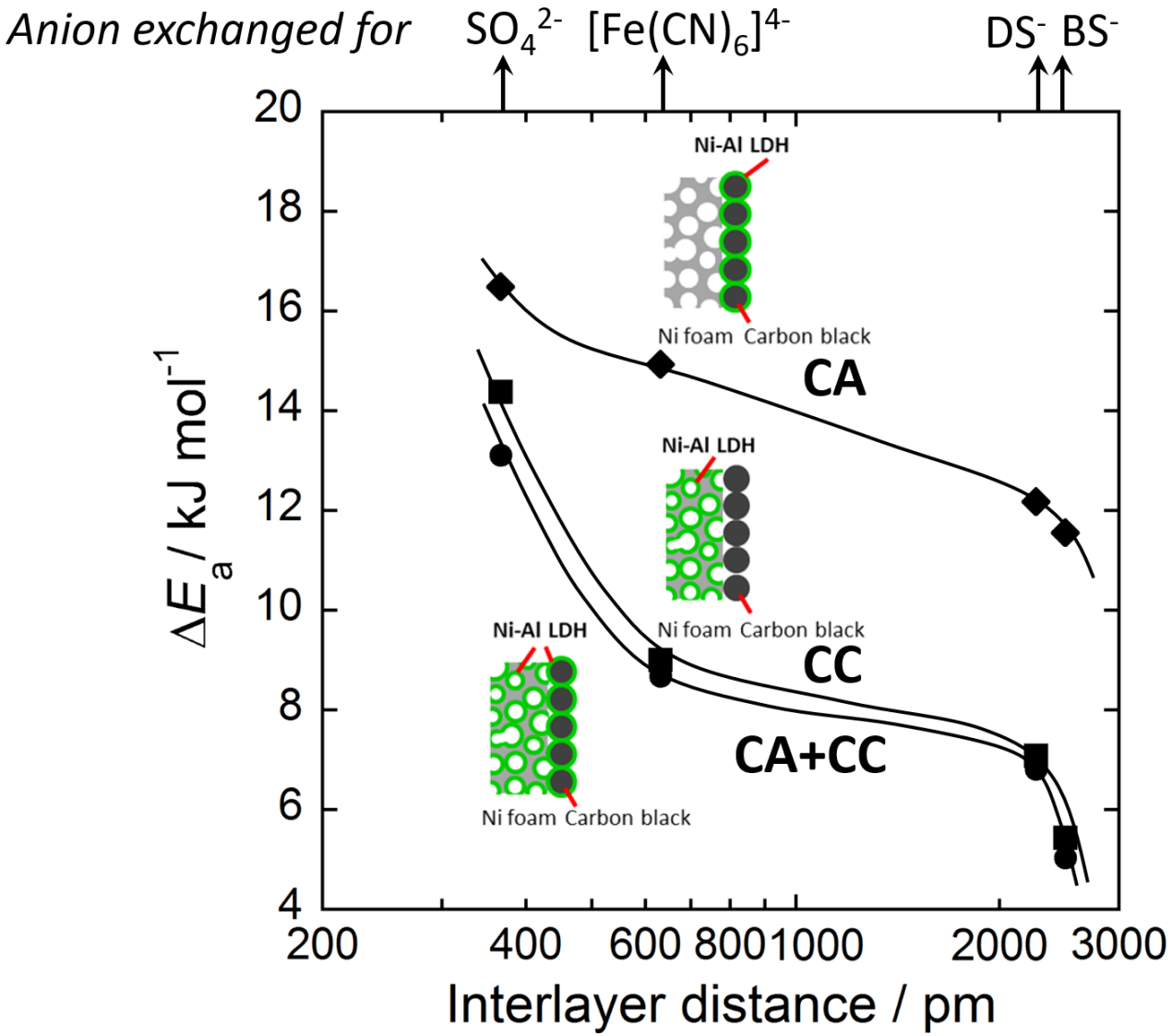

Fig. 7. Influence on anion exchange part to the Ni-Al LDH interlayer distance dependence on the apparent activation energies of the charge transfer of the electrode whose active material is the anion exchanged Ni-Al LDH. The apparent activation energies were determined using the Arrhenius equation.

Electrochimica Acta

Supplementary Material

Charge Transfer Resistance Reduction by the Interlayer Distance Expansion of Ni-Al Layered Double Hydroxide for Nickel-metal Hydride Battery Anode

Hideshi Maki[a,b*], Masayoshi Inoue[b], and Minoru Mizuhata[b]

[a]Center for Environmental Management, Kobe University, 1-1 Rokkodai-cho, Nada-ku, Kobe 657-8501, Japan

[b]Department of Chemical Science and Engineering, Graduate School of Engineering, Kobe University, 1-1 Rokkodai-cho, Nada-ku, Kobe 657-8501, Japan

*Corresponding author: maki@kobe-u.ac.jp

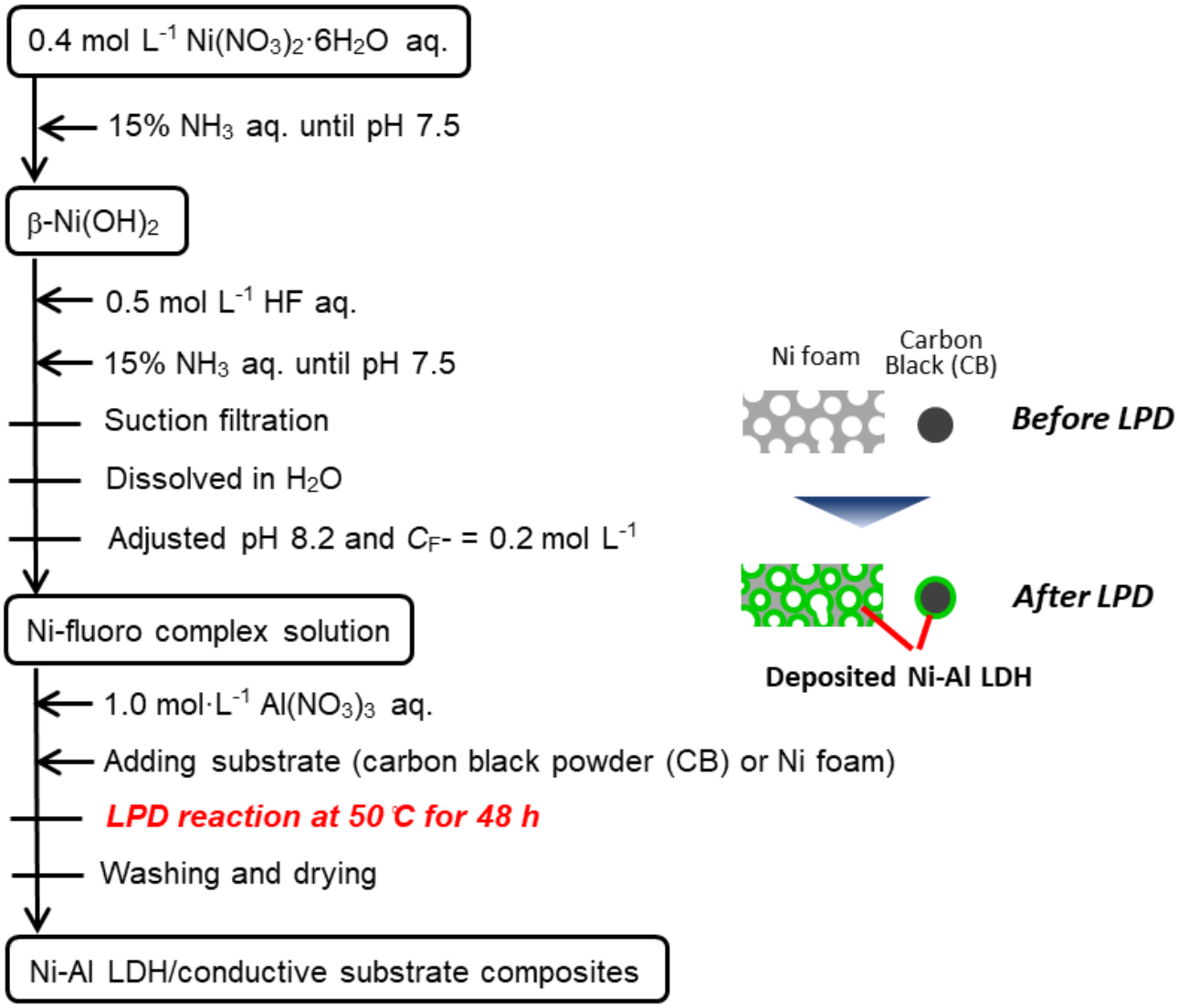

Scheme S1. Preparation of Ni-Al LDH by the LPD Reaction.

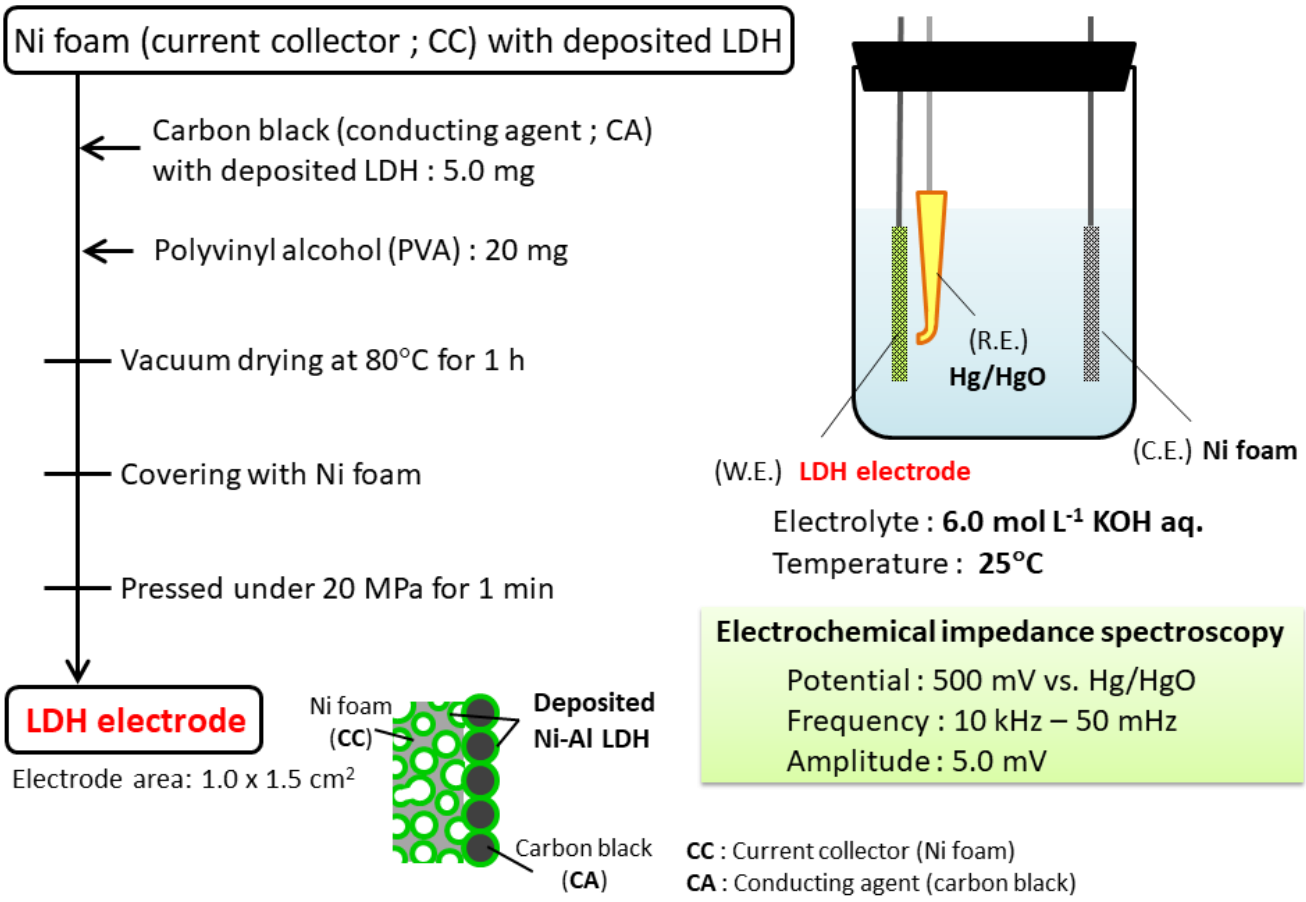

Scheme S2. Assembling of electrochemical cell and electrochemical measurements.

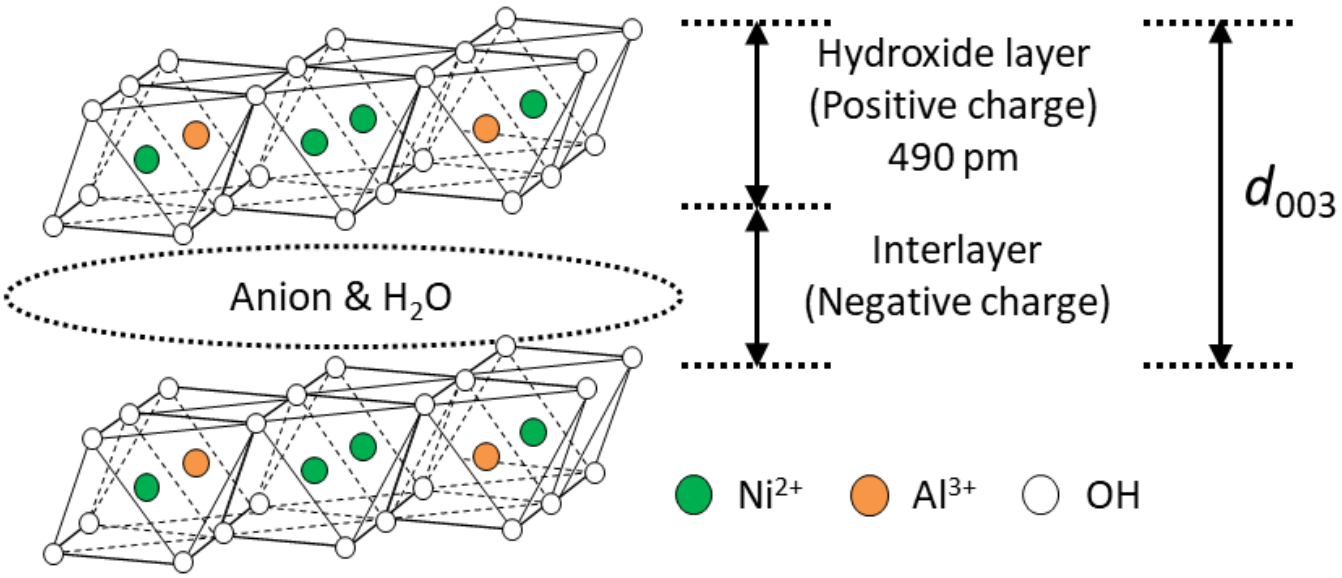

Fig. S1. Structure of Ni-Al Layered Double Hydroxide.

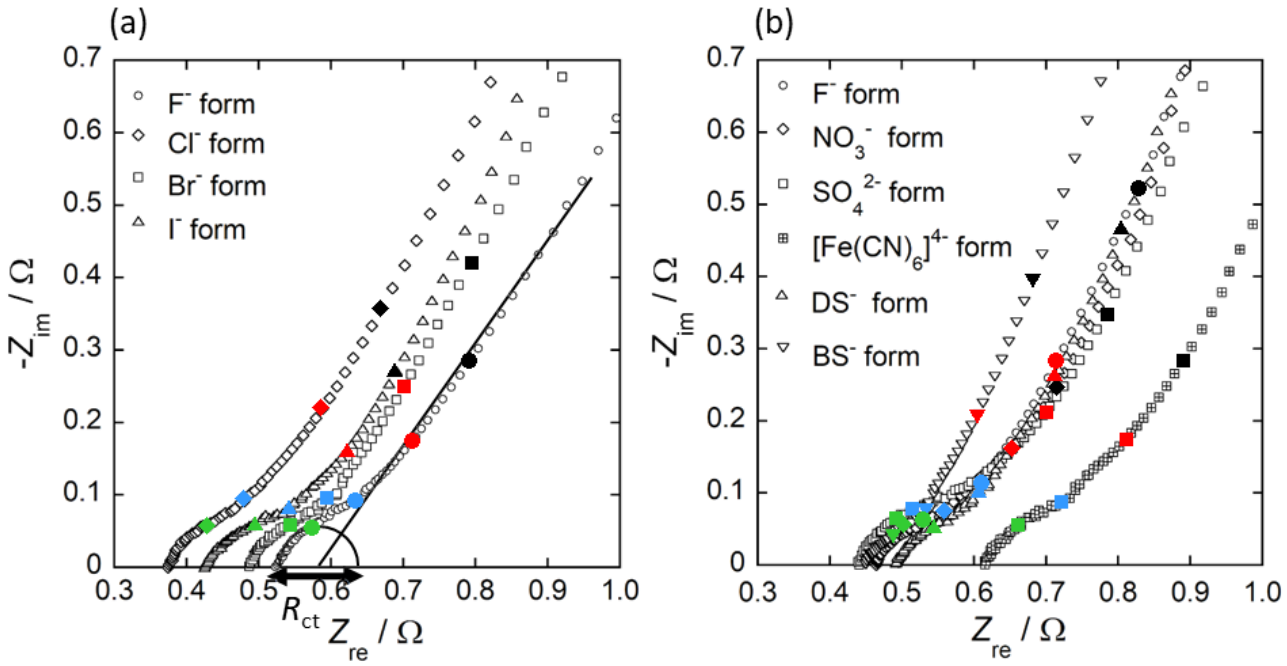

Fig. S2. Nyquist plots of the Ni-Al LDH thin films which were anion exchanged by various halide anions(a) and oxo anions, complex anions, and surface active agent anions(b). The anion exchanges were carried out for Ni-Al LDH thin films on the surfaces of both Ni foam and carbon black powder (Frequency; black: 2 Hz, red: 5 Hz, blue: 20 Hz, green: 100 Hz)).

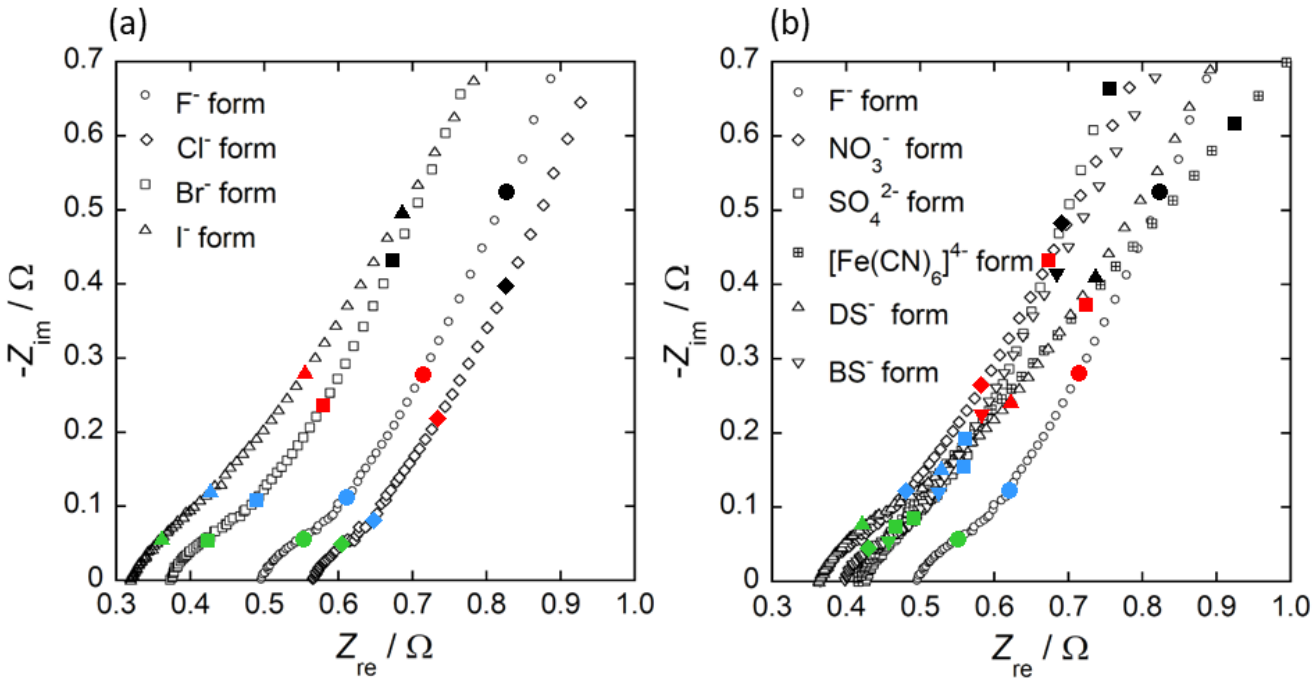

Fig. S3. Nyquist plots of the Ni-Al LDH thin films which were anion exchanged by various halide anions(a) and oxo anions, complex anions, and surface active agent anions(b). The anion exchanges were carried out for Ni-Al LDH thin films on the surface of Ni foam (Frequency; black: 2 Hz, red: 5 Hz, blue: 20 Hz, green: 100 Hz)).

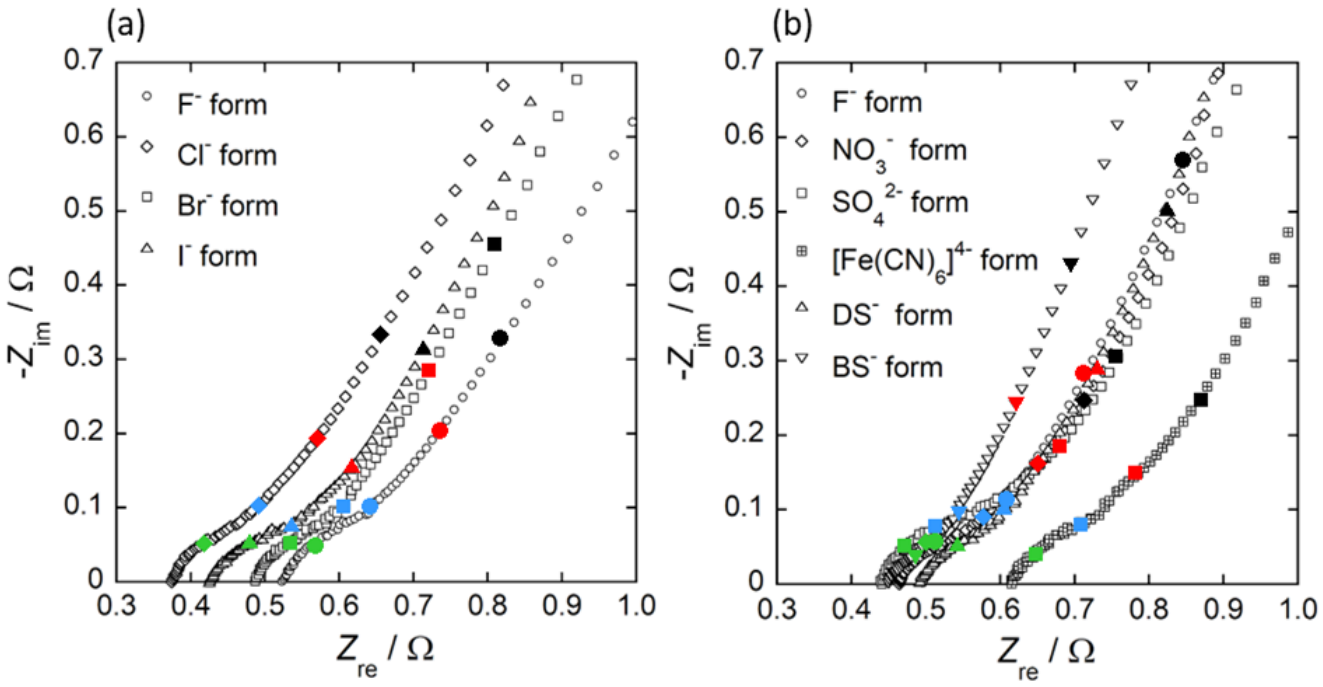

Fig. S4. Nyquist plots of the Ni-Al LDH thin films which were anion exchanged by various halide anions(a) and oxo anions, complex anions, and surface active agent anions(b). The anion exchanges were carried out for Ni-Al LDH thin films on the surface of carbon black powder (Frequency; black: 2 Hz, red: 5 Hz, blue: 20 Hz, green: 100 Hz)).

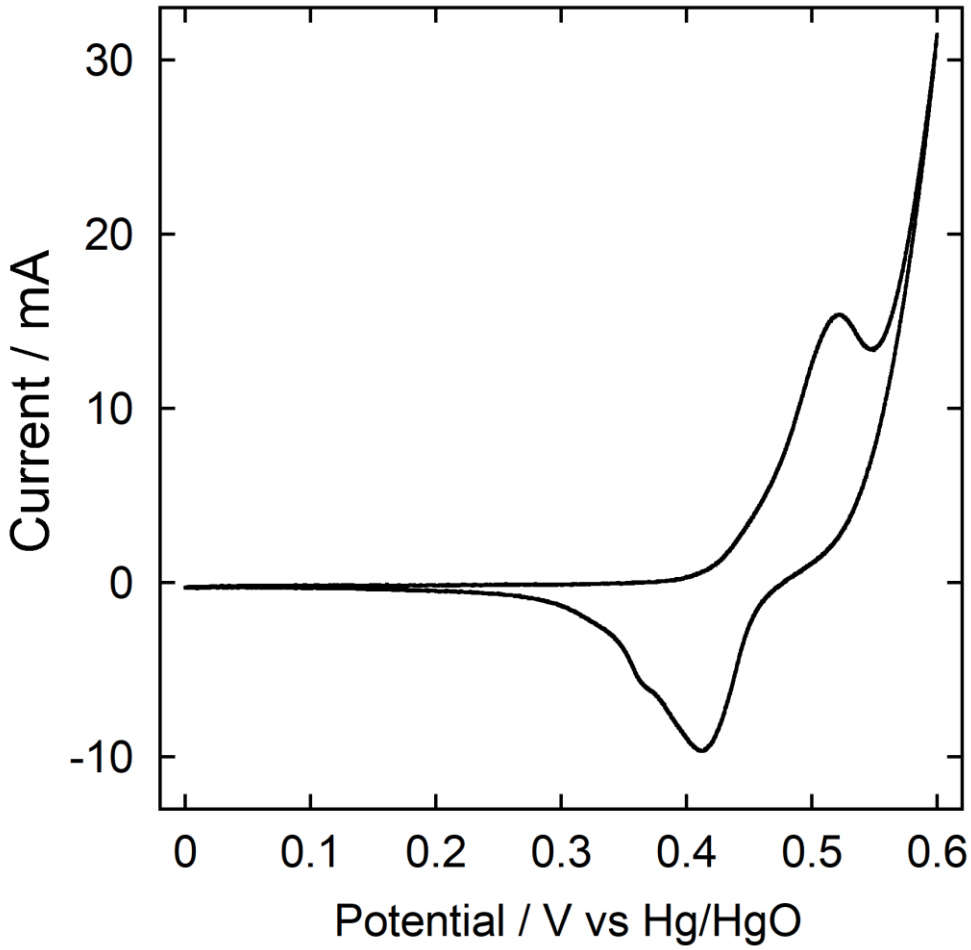

Fig. S5. CV of the Ni−Al LDH thin film which was anion exchanged by $[Fe(CN)_6]^{4-}$ anion. The anion exchange was carried out for Ni−Al LDH thin film on the surface of both Ni foam and carbon black powder.

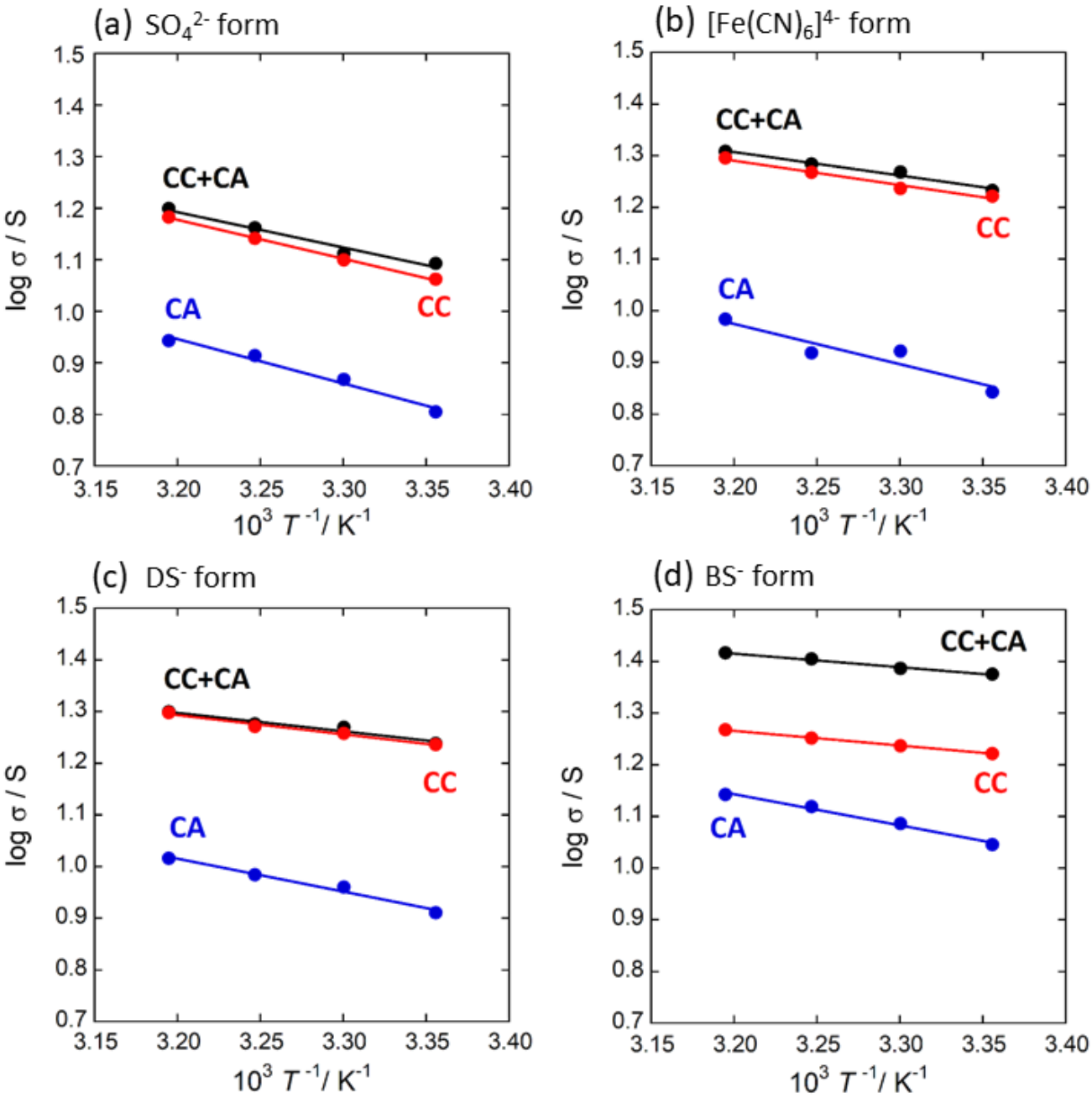

Fig. S6. Arrhenius plots for the determination of the apparent activation energies, ΔE_a, of the charge transfer in the anion-exchanged Ni-Al LDH on the surfaces of the Ni foam and/or carbon black powder.

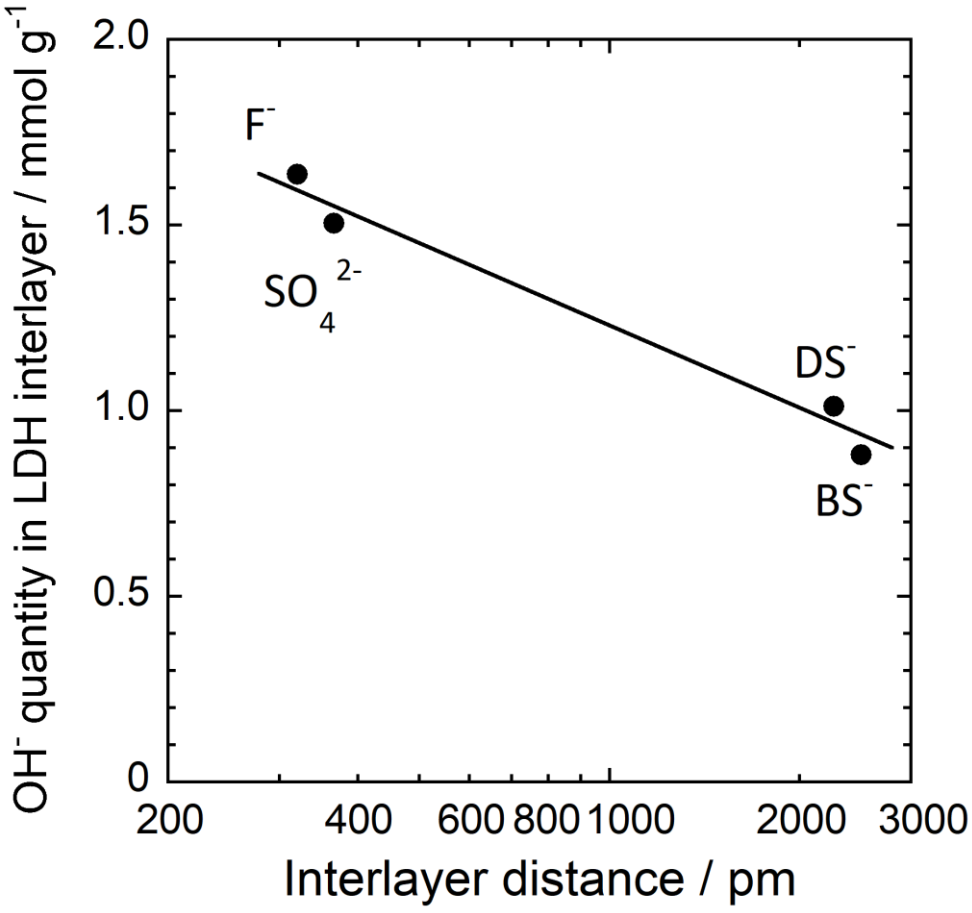

Fig. S7. OH^- quantity in the interlayer of the anion-exchanged Ni-Al LDH determined by pH titration. The as-dep. Ni-Al LDH (i.e., F^- form) and anion exchanged Ni-Al LDHs were immersed into 6 mol L^{-1} KOH aq. for 24 h, and then they were dipped into 50 mL H_2O and titrated by 0.01 mol L^{-1} HCl aq. while measuring of the pH.